



Available online at www.sciencedirect.com

SCIENCE @ DIRECT®

Journal of Hydrology 297 (2004) 174–186

Journal
of
Hydrology

www.elsevier.com/locate/jhydrol

Snowmelt infiltration: monitoring temporal and spatial variability using time-lapse electrical resistivity

Helen French^a, Andrew Binley^{b,*}

^a*Jordforsk (Centre for Soil and Environmental Research), Ås, Norway*

^b*Department of Environmental Science, Institute of Environmental and Environmental and Natural Sciences, University of Lancaster, Lancaster LA1 4YQ, UK*

Received 24 November 2003; revised 23 March 2004; accepted 1 April 2004

Abstract

More than 50% of the groundwater recharge in Norway takes place during snowmelt. Given the possible threat to groundwater quality caused by potentially rapid transport through the unsaturated zone, it is important to understand the infiltration processes that take place during snowmelt, and the factors that control the temporal and spatial variability of such processes. Here, we report on the results of an experimental study of infiltration during the snowmelt period of 2001. The study was carried out at a well-characterised field plot, close to Oslo Airport. In order to examine the spatial and temporal variability of snowmelt infiltration, a series of electrical resistivity surveys were carried out using electrodes installed below the ground surface and in shallow boreholes. The results from this time-lapse survey reveal significant changes over time, and suggest that localised infiltration takes place. The patterns of inferred increases in saturation are consistent with observed reductions in snow cover and appear to be principally controlled by variations in microtopography. Resistivity changes observed at depth, using the borehole-based electrodes, show rapid percolation through the unsaturated profile. Such behaviour is consistent with observed rapid changes in local groundwater levels. The results confirm the potential threat to groundwater quality during snowmelt and illustrate the spatial scale of processes that require adequate attention in groundwater management in vulnerable areas.

© 2004 Elsevier B.V. All rights reserved.

Keywords: Snowmelt; Resistivity; Geophysics; Infiltration; Preferential flow

1. Introduction

Seasonal ground frost greatly affects the hydrology in the Boreal zone in the Northern Hemisphere. Changing temperatures and water contents at the time of freezing affect the distribution of snowmelt water into runoff and infiltration and may affect velocities and flow patterns in the unsaturated zone.

Field experiments at Moreppen, Gardermoen, Norway during the snowmelt of 1994 and 1995 showed ponding (melt water collected on the surface) and redistribution of melt water (French and Van der Zee, 1999), even though this soil normally (under unfrozen conditions) has a high infiltration capacity. The same phenomena have also been observed by several others (Derby and Knighton, 1997; Baker and Spaans, 1997).

More than 50% of the groundwater recharge in Norway takes place during snowmelt (for example, Jørgensen and Østmo, 1990). It is important to know

* Corresponding author. Fax: +44-1524-593-985.

E-mail address: a.binley@lancaster.ac.uk (A. Binley).

how the early infiltration takes place and which factors govern the melt water transport: melting/freezing of the ground, snow and ice distribution, snow accumulation, microtopography, etc. Knowledge about these processes and their inter-linking is vital for the evaluation of risk of groundwater pollution. Physical processes occurring at cm^3 and m^3 scale near the surface, as described by Stähli et al. (1996, 1997) and Granger et al. (1984), are important controls on the flow of melt water and can also affect the hydrology at a catchment scale (response time, etc.).

According to Baker and Spaans (1997), Derby and Knighton (1997), French and Van der Zee (1999) and Johnsson and Lundin (1991), infiltration during snowmelt often occurs as focused recharge in local depressions on the surface. This may cause higher velocities through the unsaturated zone than during evenly distributed infiltration on the surface, hence producing less than optimal conditions for degradation. Higher levels of saturation and short retention time in the unsaturated zone will reduce potential for microbiological degradation. Our knowledge concerning these processes is still limited, and both simulations and field experiments are needed to improve our understanding. Most hydrological models have poorly developed routines for soil freezing and thawing, hence they cannot address the extreme but common hydrological events (Flerchinger and Seyfried, 1997). Although the thermal part has been addressed, water flow in freezing and thawing systems has not been incorporated sufficiently as yet. A problem with many of the models which do include winter routines such as SOIL (Jansson, 1991), FROST (Benoit, 1974; Benoit and Mostaghimi, 1985) and SHAW (Flerchinger and Saxton, 1989) is that they are 1D and hence cannot take account of the spatial variability of the physical conditions. Some newer models have included thermal transport and phase change (Ippisch, 2001; White and Oostrom, 2000), this is, however, far from standard in most hydrogeological models.

Oslo airport, Gardermoen, is situated on Norway's largest unconfined aquifer, which consists of coarse sandy sediments. It is therefore during snowmelt and after heavy rains that the risk of pollution of the groundwater caused by airport operations, de-icing for example, is the greatest. The horizontal distribution of ground frost and basal ice at the bottom of snow pack

can cause focused infiltration in specific areas, which in turn can influence the retention time in the unsaturated zone and hence the danger of contaminating the groundwater. Water flow and chemical transport in the unsaturated zone at a field site, Moreppen, located in the vicinity of the western runway at Oslo airport (see Fig. 1), had previously been characterised by the means of 30 suction cups (French et al., 1999, 2001) and in combination with electrical resistivity tomography (French et al., 2002). Previous experiments using melting plates (0.25 m by 0.2 m) placed underneath the snow cover to collect melt water, showed a large spatial variability of snowmelt, which was strongly correlated with microtopography (French and Van der Zee, 1999). This technique, however, did not provide information about the actual infiltration that took place. Time domain reflectometry and neutronmeters have been used to characterise infiltration during snowmelt (Langsholt et al., 1996) but both techniques provide limited spatial information. In order to address this limitation we show here how geophysical

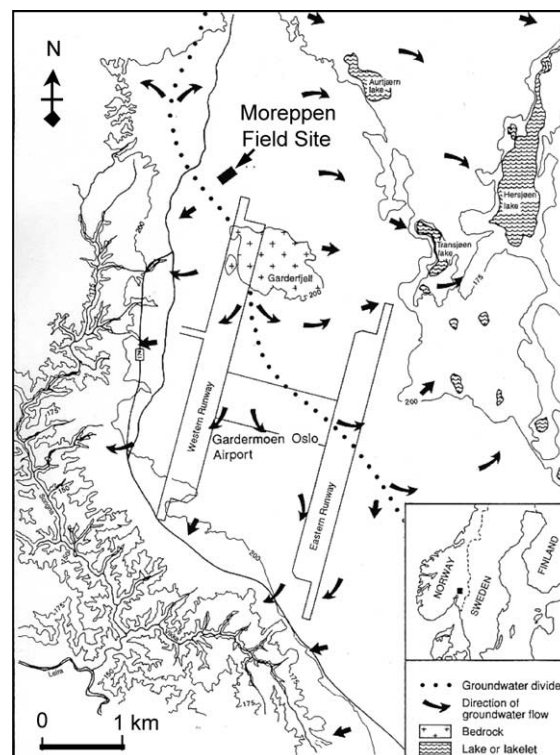


Fig. 1. Location of Moreppen field site.

measurements may be used to determine spatial variability of infiltration during snowmelt processes.

The geophysical method selected for our experiment is electrical resistivity, using surface and borehole deployed electrodes. In our set-up the technique provides time series of 3D images of the resistivity distribution in a 60 cm deep volume. The resistivities are functions of soil structure, water content and pore water conductivity. In a melting partly frozen soil, water contents will change because of infiltrating melt water. A combination of geophysical and hydrological techniques performed at the same site during an electrolyte tracer experiment at Moreppen during the snowmelt of 2001, showed that electrical resistivity imaging could serve as a valuable supplement or replacement monitoring system for flow and transport in the unsaturated zone during snowmelt in this type of environment (French et al., 2002). The objective here is to quantify the spatial and temporal variability of the infiltration pattern during snowmelt and to relate that to microtopography, snow cover, and temperature on the surface. The questions we pose are: does infiltration during snowmelt vary spatially over length scales of a few metres? If so, what factors control such variability?

2. Experimental methods

2.1. The field site

The fieldwork for this experiment was carried out at Moreppen, Gardermoen (French et al., 1994) in south-eastern Norway. The Gardermoen glacial-contact delta is an aquifer composed of sand and gravel underlain by silty glaciomarine deposits (Jørgensen and Østmo, 1990; Tuttle, 1997). The unsaturated zone (1–30 m thick) is heterogeneous with sediments of fine to coarse sand and gravel. The unsaturated zone at the field site mainly consists of coarse sandy soil with heterogeneous layers of varying grain size distribution from fine sand to coarse gravel with stones. In its natural state, the ground surface is mostly forested (mainly spruce) with open areas of pioneering vegetation (grass, bushes, young birch).

The annual precipitation is approximately 800 mm and the evapotranspiration is about 400 mm. About 50% of the groundwater recharge occurs during the (3–5 weeks) snowmelt period (Jørgensen and Østmo, 1990). Fig. 2 shows measured snowmelt and rainfall during April 2001 (the period of study for the geophysical surveys reported here). Also shown in

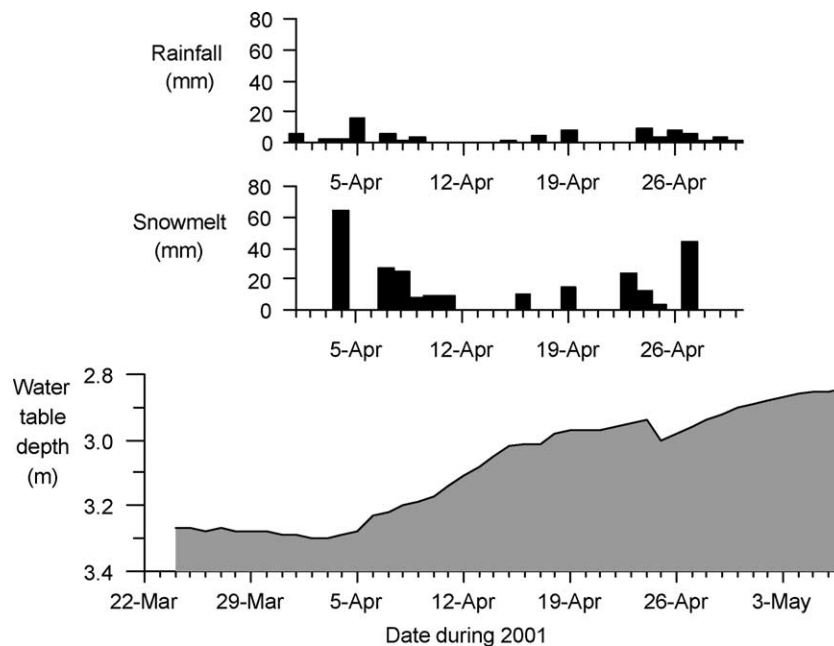


Fig. 2. Snowmelt and rainfall at the field site during April 2001 and observed changes in groundwater level.

Fig. 2 is a groundwater hydrograph measured at the site. The water table clearly responds rapidly to the first snowmelt event on 4 April 2001, and the significant change in groundwater storage supports the earlier findings of Jørgensen and Østmo (1990) noted earlier.

2.2. The experimental set-up

An area 4 m by 6 m, situated between two patches of trees, was selected for studies of surface processes during the snowmelt of 2001. The area is fairly flat (elevation differences of about 20 cm) and consequently it is logical to assume uniform infiltration over the area. In Fig. 3, a plan of the experimental plot shows the location of temperature sensors, near surface electrodes and borehole electrode arrays. Installation at the site took place during the autumn of 2000. This autumn was extremely wet and freezing temperatures occurred in mid December, some weeks prior to snow fall. Temperature cells were placed on the soil surface, in between the vegetation, to monitor temperatures underneath the snow cover (see Fig. 3). To indirectly monitor changes in water content near the surface, 6 lines (3.75 m long) of 16 electrodes (separated by 0.25 m) were placed in one corner of the defined area. The 96 electrodes, made of stainless steel mesh, were installed at 20 cm depth by inserting them through small holes (1 cm in diameter) to

minimize the disturbance of the surface. Four boreholes, labelled TEL1, TEL2, TEL3 and TEL4, were installed, each with a set of 16 stainless steel mesh electrodes mounted, at 0.16 m intervals, on a 4 cm diameter PVC pipe. The top electrode is situated near the surface, the bottom electrode at a depth of 2.4 m.

Snow melting was monitored at the site by measuring changes in snow depth (including snow water equivalents) and by collection of melt water from melting plates (French et al., 1999). White measuring sticks were placed in each corner, and in the centre of the defined area prior to the snowfall, to monitor the change in snow depth throughout the snowmelt. The water equivalent in the snow was measured at several locations on the site throughout the experiment to keep track of the water storage in the snow pack above the experimental site. A lysimeter trench approximately 10 m from the surface monitoring site was used to monitor vertical variation in soil temperatures, from 0.05 m down to 2.4 m, and to monitor tracer movement in the unsaturated soil during snowmelt in a companion experiment (reported in French et al., 2002). The groundwater depth was logged hourly throughout the period. Photographs taken from a small hill approximately 5 m from the monitored site documented the horizontal distribution of snow cover. The oblique photos were transformed to ortho-photos, using PhotoModeler 3.1 (EOS systems 1999) reported in Kjeldset (2002).

2.3. Electrical resistivity surveys

Electrical resistivity data were collected on a regular basis from 25 March 2001, before snowmelt had started, until 4 May, some days after all the snow had melted. Thus, changes in the resistivity distribution, caused by the infiltration of water, could be imaged as a function of time. Electrical resistivity was measured in a Wenner configuration (see for example, Reynolds, 1997) in both the surface and borehole electrode arrays. The data set collected 1 April was used as the background image for the surface lines, while 28 March was used as the background dataset for the borehole Wenner surveys.

For all resistivity surveys, reciprocity (the current and potential electrodes are swapped for each

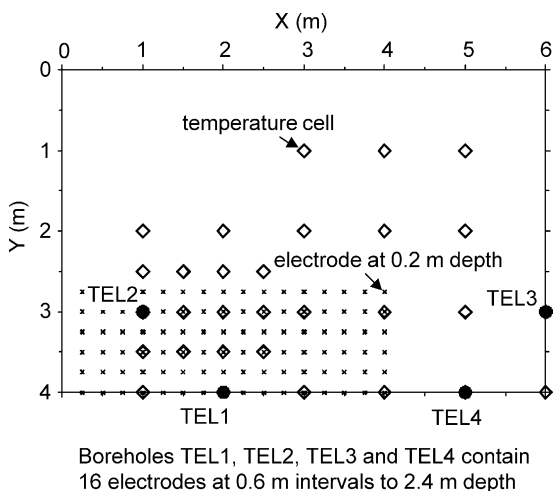


Fig. 3. Layout of experimental plot. Boreholes TEL1, TEL2, TEL3 and TEL4 each contain 16 electrodes at 0.6 m intervals to 2.4 m depth.

configuration, see for example, Binley et al., 1995) of every measurement was checked. To prevent misinterpretation of artefacts, measurements with reciprocity errors greater than 10% were removed from the data sets prior to any inversion of the resistivity data. Datasets containing a common set of measurement for the whole time period were then produced to ensure the image sensitivity is not biased by different measurements. The surface array data were processed using a 3D inverse solution in order to determine a distribution of resistivities that are consistent with the measured data. The procedure adopted here was the well-established 'Occams' approach (see for example, LaBrecque et al., 1996). A finite element grid consisting of approximately 108,000 elements was used with reasonably fine discretization within the region of the arrays using elements 6.25 cm (long) by 6.25 cm (wide) by 5 cm (deep). The mesh was parameterised into 13,000 parameter blocks, 1800 of which lie in a region 3.75 m (long) by 1.25 m (wide) by 0.6 m (deep) that was extracted for interpretation.

For the borehole arrays, measured electrical resistance data were converted to apparent resistivities (see Telford et al., 1990) using appropriate geometric factors that accounted for the position of the electrode in the borehole and the spacing of the electrodes.

The result, at each survey date, was a resistivity profile between the ground surface and 2.4 m.

3. Results and discussion

3.1. Change in snow cover

On 19 April 2001 the experimental plot had 100% snow cover. In Fig. 4 the change in snow cover, determined from the photographs, from April 23 until April 27 is displayed, indicating the fast melting activity during this period. The percentage area covered by snow over the experimental plot in April is also shown in the same figure. The estimated reduction in water equivalent in the snow cover during the same period (19–27 April) was 132 mm. By 1 May all the snow had melted. Soil temperatures near the surface are strongly affected by snow cover, as expected. In Fig. 5 the average soil temperature and range, established from the 29 temperature cells, is shown for the month of April. The time series illustrates the relatively stable temperature prior to 20 April and the subsequent variability (peaks) following removal of snow cover. A similar pattern was seen for soil temperatures measured at different depths: French et al. (2001) show temperature series

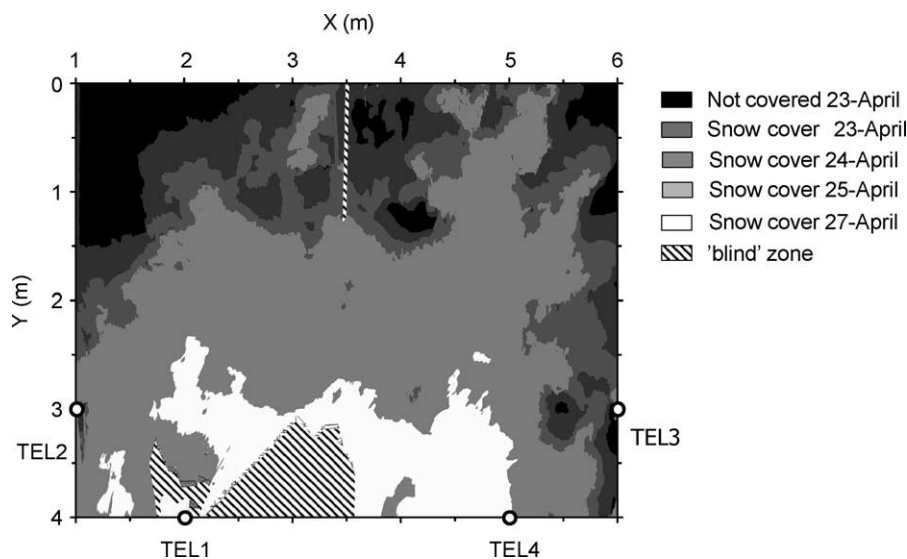


Fig. 4. Horizontal distribution of snow-cover from 23 April until 27 April determined from photographs. The whole area was covered on April 19 and all the snow had melted by 1 May.

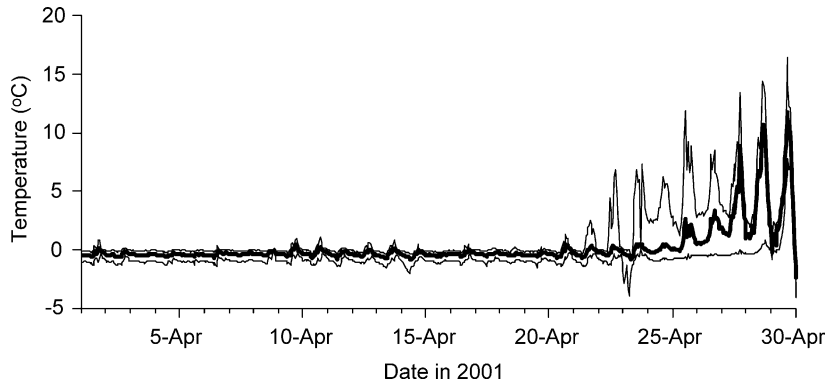


Fig. 5. Changes in soil temperature during April 2001. The heavy line shows the average temperature for the 29 temperature cells. The light lines show the temperature range in the array of the cells. The peaks indicate complete melting of snow.

at depths of 0.1, 0.4 and 0.9 m at a site 10 m from the plot under study here. It is apparent from these data that the soil temperatures did not start to increase until the snow and ice cover had gone (see Fig. 6). From this we assume that the soil below the site was frozen

through most of April, and that percolation took place through the frozen layer. It is the ice layer on the ground surface that is mostly responsible for the redistribution of melt water. The formation of basal impermeable ice may be due to the freezing

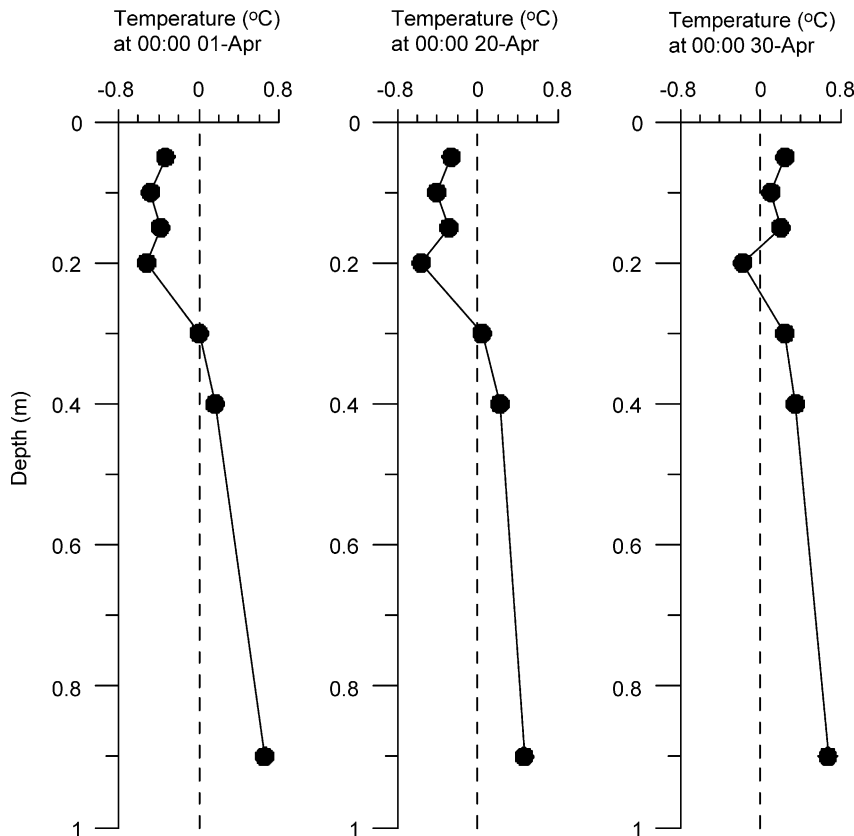


Fig. 6. Soil temperature profiles on 1 April, 20 April and 30 April measured 10 m from the field plot.

and thawing processes in the near surface (top few centimetres) sediments. Even in a detailed model, such as SOIL (Jansson, 1991), where soil freezing conditions are included, this process is not described well (S. Kværnø, pers. comm.).

3.2. Changes in borehole resistivity profiles

Resistivity of the soil will change over time due to varying soil moisture content and soil water conductivity. Soil water conductivity will change as ionic concentration and temperature varies. We assume here that the changes in ionic concentration are insignificant and that during most of the survey period soil water temperature is stable (as shown in Fig. 5). Resistivity changes will thus be principally controlled by changes in volumetric water content. Note also that, as the snow pack melts, the surface boundary condition changes (electrically) and, if the change is significant, it must be incorporated within

the electrical potential (forward) modelling algorithm. However, since the snow pack will be much more resistive than the soil, the effect of the snow pack thickness can be ignored.

Fig. 7 shows the changes in resistivity, relative to 28 March, observed in the four borehole arrays. In all arrays a maximum change of over 60% is observed, indicating a significant change in the water content of the soil. The change in ground surface inputs are also shown in Fig. 7 to aid interpretation of the resistivity time series. Large changes in resistivity in boreholes TEL1 and TEL2 coincide with a sharp increase in snowmelt at the site on 15 April. The borehole profiles also suggest variability in infiltration over distances of a few metres; profiles in TEL3 and TEL4 (approximately 1.4 m apart) are very similar but markedly different from those determined in TEL1 and TEL2. Perhaps more significant is the rapid changes at depth in all boreholes, in particular TEL1. Such an observation is consistent with the fast reaction of the water table to

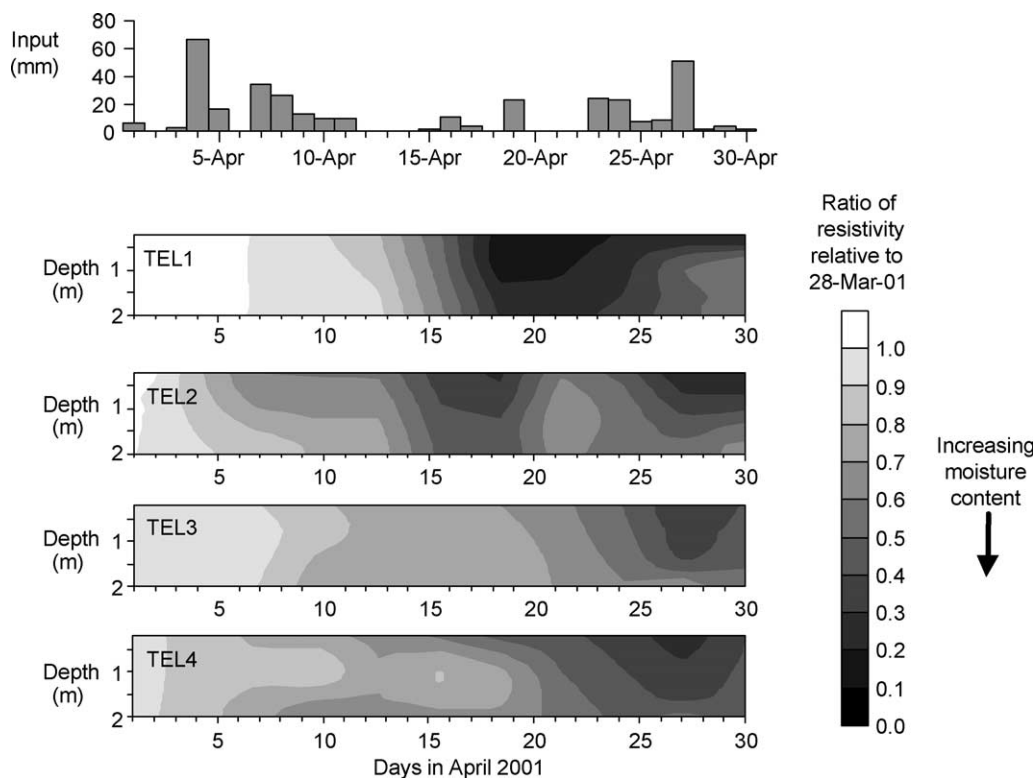


Fig. 7. Changes in apparent resistivity in the borehole electrode arrays. The total (snowmelt and rainfall) inputs at the site are also shown for comparison.

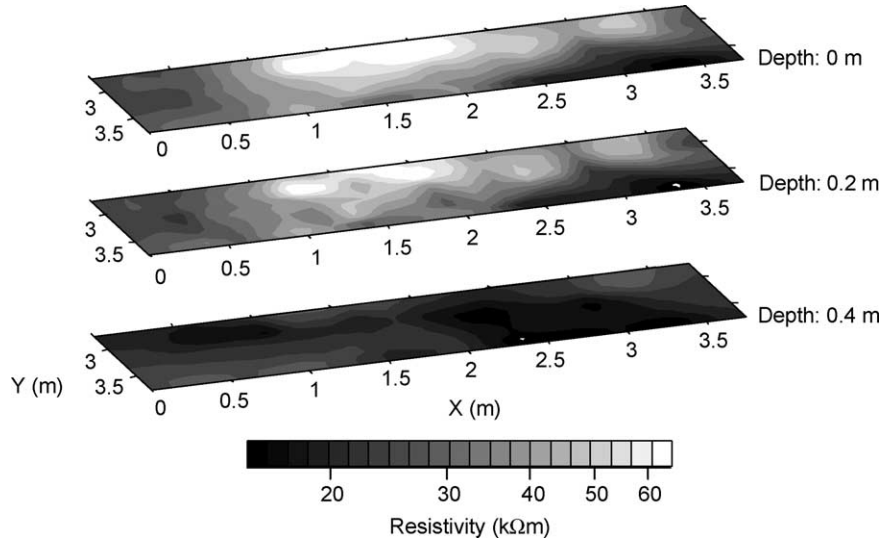


Fig. 8. Horizontal slices in the 3D image of resistivity determined from the pre-snowmelt image (1 April 2001). Slices at depths of 0, 0.2 and 0.4 m are shown.

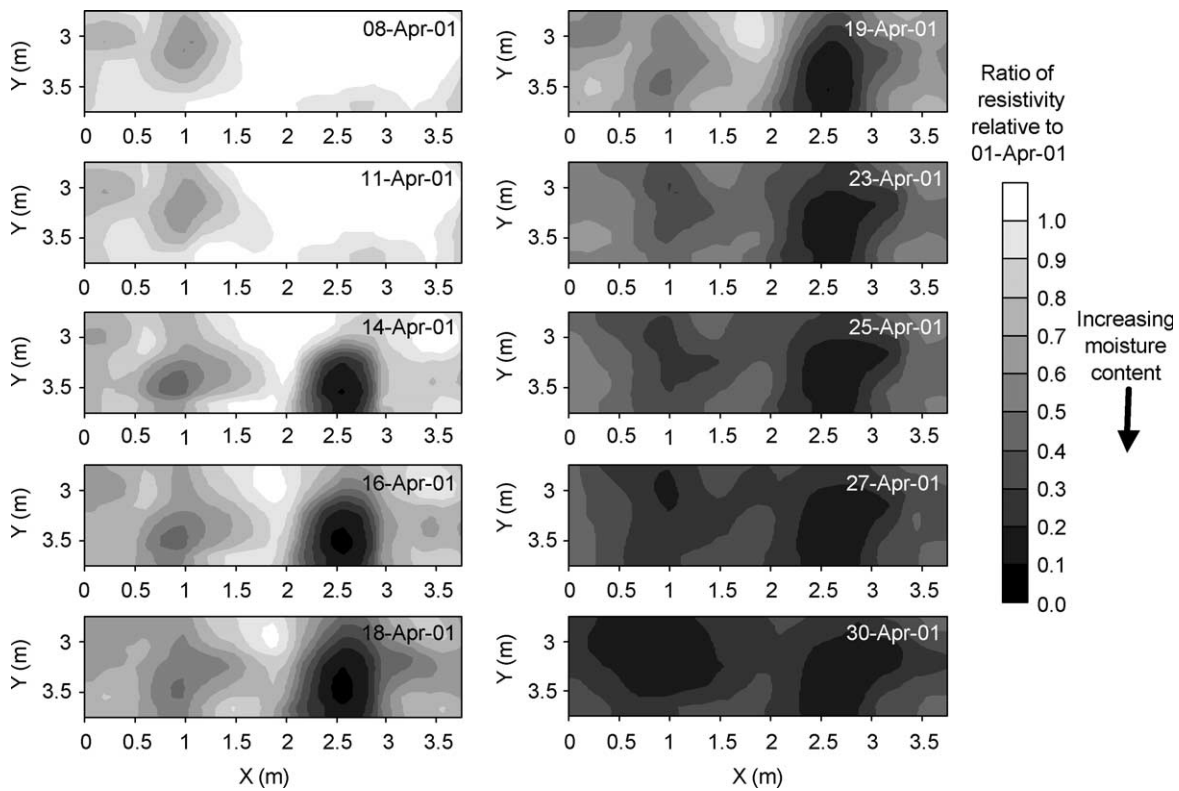


Fig. 9. Changes in resistivity at the soil surface based on electrical resistivity normalised on initial conditions on 1 April 2001.

inputs, as shown in Fig. 2. A small pond, approximately 1m in diameter, was formed about 0.5 m from TEL1, just outside the monitored area. This pond started forming around 11 April and was completely drained by 24 April, and may have influenced the particularly fast response at this location.

3.3. Changes in 3D resistivity images

Horizontal slices from the pre-snowmelt 3D resistivity image taken on 1 April is shown in Fig. 8. The high resistivity values reflect the low moisture retention capacity of the soil and the low pore water electrical conductivity. Previous surveys close to the site (see French et al., 2002) observed resistivities in the range 50–200 k Ω m and pore water conductivities in the range 20–30 μ S/cm. Variation in resistivity near the surface will also be influenced by variability in the thickness of the near surface

frozen layer, although surface temperatures measured above the electrodes at the time were all near 0 °C (see Fig. 5). Typically the seasonal soil frost at this site is about 0.4 m during winter (French and Van der Zee, 1999; French et al., 2002).

The sequence of images in Fig. 9 shows the changes in the resistivity distribution with time in the surface plane, extracted from the 3D resistivity images. The infiltration pattern displayed in Fig. 9 is heterogeneous and does not have any apparent relation to the initial conditions displayed in Fig. 8. In Fig. 9, two locations of focussed infiltration within the area monitored by the surface lines are observed (locations: $X = 2.5$ m, $Y = 3.5$ m and $X = 1$ m, $Y = 3.25$ m). By 14 April these two zones dominate the changes near the surface. From 19 April other areas in the plot respond and by the end of the snowmelt period the entire plot shows more uniformity in the change in resistivity. It is interesting

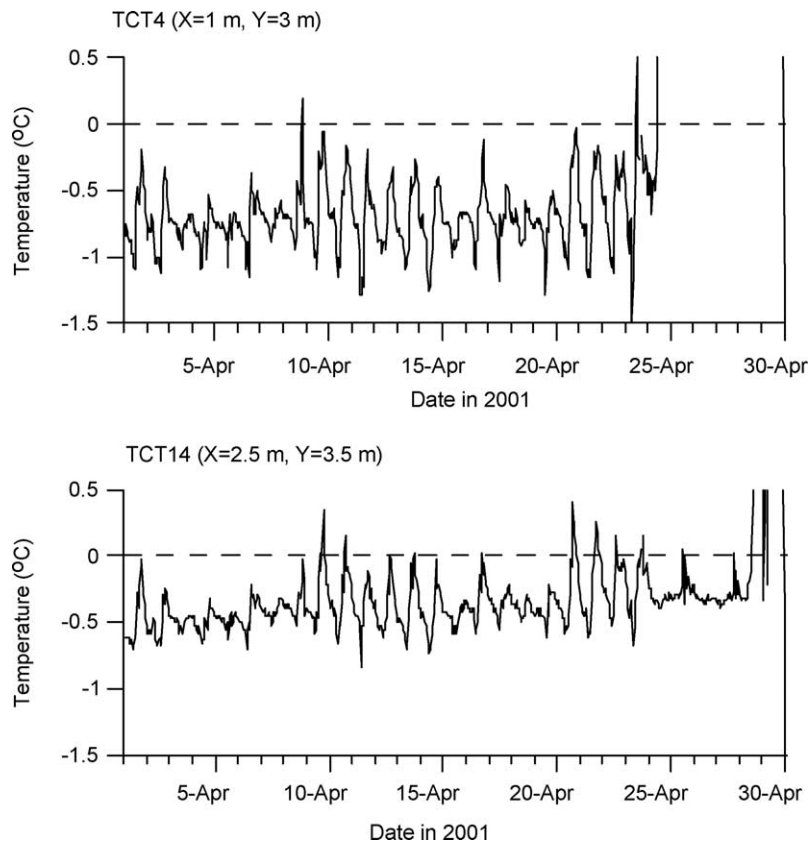


Fig. 10. Variation in soil temperature in temperature cells TCT4 and TCT14.

to note that the large changes in resistivities early in the snowmelt are not clearly reflected on the surface, for example in the snow cover. Apart from the melt water ponds scattered around the Moreppen field site, very little variability was seen on the surface until 23 April (see Fig. 4).

Fig. 10 shows soil temperature variation during April, recorded in two temperature cells TCT4 and TCT14. TCT4, located at $X = 1$ m, $Y = 3$ m, shows a short period of thawing on 9 April, followed by a period of freezing until 24 April. This correlates well with the periods of increases in level of saturation inferred from the resistivity changes shown in Fig. 9: at location TCT4, a localised reduction in resistivity occurs on the 8 April and 11 April images and does not reappear until 23 April. In contrast, TCT14, located at $X = 2.5$ m, $Y = 3.5$ m, shows a prolonged period of thawing conditions after 10 April. At the location of TCT14, the resistivity is seen to reduce progressively after 14 April (see Fig. 9).

The 3D variability of resistivity within the plot is also shown in Fig. 11, for selected dates. Here, only changes over 70% are shown in order to reveal the variability at depth. Archie’s Law (see, for example, Reynolds, 1997) relates the soil’s resistivity (ρ_s) to the soil’s saturation (S), porosity (ϕ), and pore fluid resistivity (ρ_w) as follows

$$\frac{\rho_s}{\rho_w \phi^{-m}} = S^{-n}, \tag{1}$$

where the exponents m and n in Eq. (1) are empirically derived constants. Given that we are primarily interested in changes and that porosity is unlikely to change, we can derive the following equation:

$$\frac{S_t^{-n}}{S_{t=0}^{-n}} = \frac{\rho_{w,t=0} \rho_{s,t}}{\rho_{w,t} \rho_{s,t=0}}. \tag{2}$$

The subscripts $t = 0$ and t indicate conditions before and after the soil’s property change due to fluid invasion.

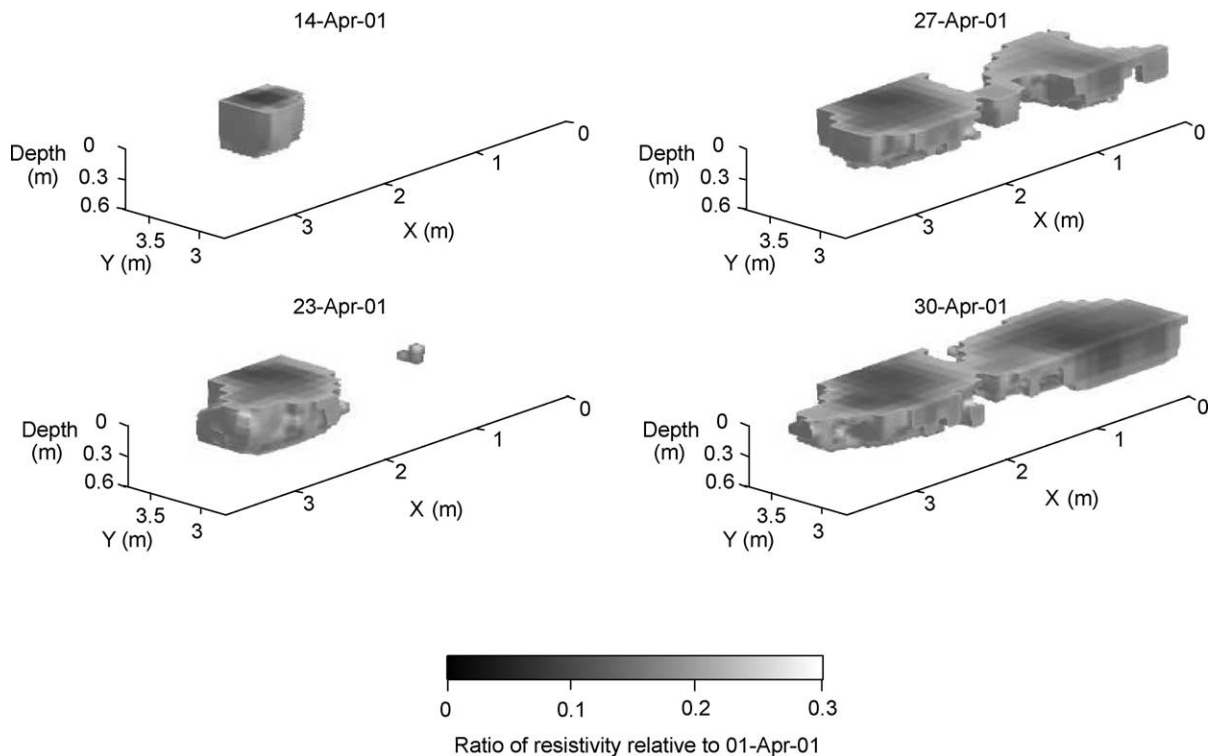


Fig. 11. Changes in resistivity relative to 1 April 2001 within the 3D imaged volume, at selected times.

If we assume that the pore water conductivity does not change, then:

$$\frac{S_t}{S_{t=0}} = \left[\frac{\rho_{s,t}}{\rho_{s,t=0}} \right]^{-1/n} \quad (3)$$

Knowledge of parameter n and the change in resistivity permits computation of the change in saturation. If we assume $n = 2$, for purpose of illustration (but see also Reynolds, 1997), then a reduction in resistivity of 70% is equivalent to an increase in saturation of 80%.

Fig. 12 shows how the fraction of surface area in which resistivity changes are significant varies during the snowmelt period. Here, 70% is used as a somewhat arbitrary threshold and is equivalent to an increase in saturation of 80% or above, assuming the Archie relationship described above. Between 11 April and 23 April, a steady increase in the surface

area of the plot (within the surface electrode arrays) that experiences a reduction in resistivity of 70% or above is seen. By 23 April the ‘percentage significantly infiltrated area’ is only approximately 20%. After this date, changes are more rapid.

3.4. Topographic control on infiltration

The changes in resistivity reported above suggest that at the experimental site (1) infiltration during early stages of snowmelt is localised and (2) variation in moisture content at depth is rapid. Microtopography has previously been proposed as a controlling factor on such highly variable infiltration during snowmelt (French and Van der Zee, 1999). As shown in Fig. 13, topographic variation within the experimental plot reveals two local depressions that are located in the areas where significant changes in resistivity were observed. It would appear that

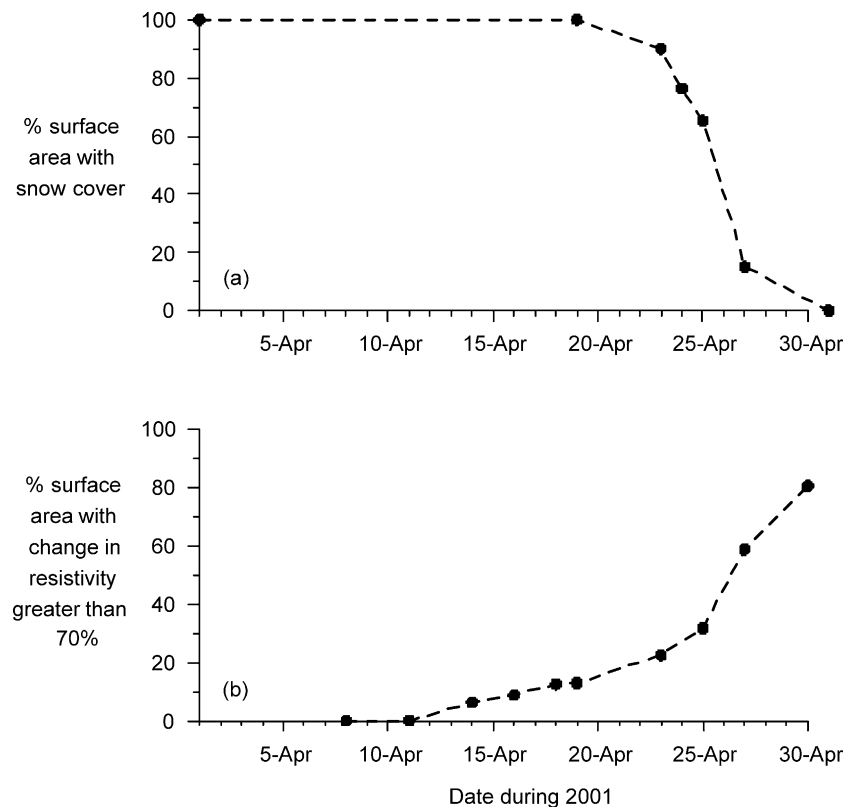


Fig. 12. (a) Changes in percentage snow cover and (b) variation in percentage surface area, during the snowmelt period, experiencing changes in resistivity above 70%.

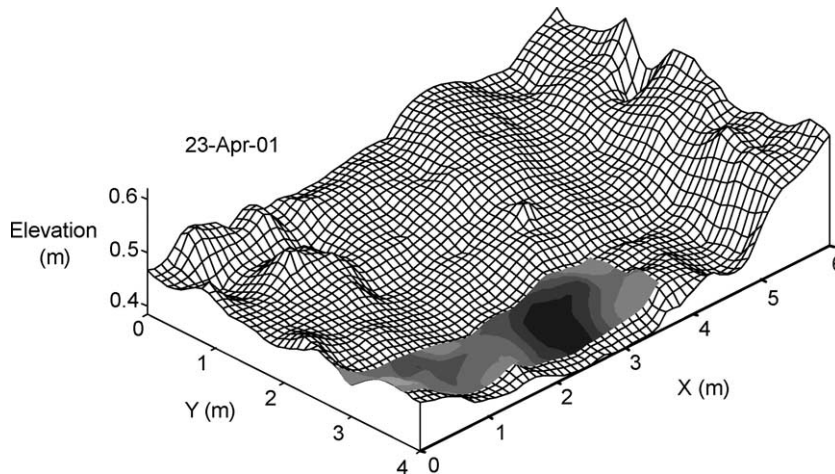


Fig. 13. Variation in microtopography in the experimental plot, overlain with the changes in resistivity between 1 April and 23 April 2001.

although these areas retain snow cover towards the end of the snowmelt period (see Fig. 4), melt water from surrounding snowpack drains towards these regions, controlled by topographic variability, and promotes infiltration into the soil.

4. Conclusions

The results of a time-lapse geophysical survey during the snowmelt period of 2001 suggest that spatial variability of snowmelt infiltration is strongly influenced by microtopography. Borehole-based measurements reveal evidence of rapid percolation towards the water table. Changes in soil water saturation are smoothed out, to some extent, as water percolates. This is supported by earlier simulations with variable infiltration into a heterogeneous soil. Ponds, however, can have a much larger effect on the infiltration pattern, and locally give extremely large and fast changes in water content. The area that takes part in the infiltration increases throughout the melting period, that is, the available melt water early in the snowmelt is forced through a small portion of the surface area. The elevated, albeit localised, saturation implies that transport of potential pollutants may occur at higher velocities than through a uniform system.

A time-lapse electrical resistivity survey appears to be a useful method for monitoring the infiltration process during heterogeneous melting conditions.

If snow contains pollutants that may affect the electrical conductivity of the melt water, it would be necessary to include methods for separation of effects of water content and water conductivity changes, for example, using local (point) measurements of water content and conductivity. Time domain reflectometry data, for example, would serve as useful supplementary local measurements in this respect.

We believe that geophysical methods offer the potential for improving models of snowmelt infiltration processes because of the high data (spatial and temporal) density and minimally invasive nature of the measurements. Geophysical images of moisture content changes may be utilised for deterministic model calibration (as illustrated recently in a study of vadose zone flow by Binley et al., 2002), however, they may also offer the means of investigating geostatistics of dynamic processes. As a result, geophysics may create the potential for modelling processes at a range of scales and allow the results from small field scale studies to be interpreted at the regional scale.

Acknowledgements

This research was funded by the Norwegian Research Council (project no. 138510/410). The authors thank Carol Hardbatt, Cathrine Waage Tveit, Leif Jakobsen and Peter Winship for their considerable contribution with the collection of field

data. We also thank D.L. Kane and an anonymous reviewer for their constructive comments on an earlier version of the manuscript.

References

- Baker, J.M., Spaans, E.J.A., 1997. Mechanics of meltwater movement above and within frozen soil. In: Iskandar, I.K., Wright, E.A., Radke, J.K., Sharratt, B.S., Groenvelt, P.H., Hinzman, L.D. (Eds.), *International Symposium on Physics, Chemistry, and Ecology of Seasonally Frozen Soils*, US Army Cold Regions Research and Engineering Laboratory, Fairbanks, Alaska, 10–12 June, pp. 31–36.
- Benoit, G.R., 1974. Frost depth and distribution from heat flow model. *Proceedings of the Eastern Snow Conference* February 7–8, pp. 123–144.
- Benoit, G.R., Mostaghimi, S., 1985. Modelling soil frost depth under three tillage systems. *Trans. ASAE* 28, 1499–1505.
- Binley, A., Ramirez, A., Daily, W., 1995. Regularised image reconstruction of noisy electrical resistance tomography data. In: Beck, M.S., Hoyle, B.S., Morris, M.A., Waterfall, R.C., Williams, R.A. (Eds.), *Process Tomography—1995*, Proceedings of the 4th Workshop of the European Concerted Action on Process Tomography, Bergen, 6–8 April, pp. 401–410.
- Binley, A., Cassiani, G., Middleton, R., Winship, P., 2002. Vadose zone model parameterisation using cross-borehole radar and resistivity imaging. *J. Hydrol.* 267, 147–159.
- Derby, N.E., Knighton, R.E., 1997. Frozen soil effects on depression focused water and solute movement. In: Iskandar, I.K., Wright, E.A., Radke, J.K., Sharratt, B.S., Groenvelt, P.H., Hinzman, L.D. (Eds.), *US Army Cold Regions Research and Engineering Laboratory; International Symposium on Physics, Chemistry, and Ecology of Seasonally Frozen Soils*, Fairbanks, Alaska, 10–12 June, pp. 113–119.
- Flerchinger, G.N., Saxton, K.E., 1989. Simultaneous heat and water model of a freezing snow-residue-soil system 1. Theory and development. *Trans. ASAE* 32(2), 565–571.
- Flerchinger, G.N., Seyfried, M.S., 1997. Modeling soil freezing and thawing, and frozen soil runoff with the shaw model. In: Iskandar, I.K., Wright, E.A., Radke, J.K., Sharratt, B.S., Groenvelt, P.H., Hinzman, L.D. (Eds.), *International Symposium on Physics, Chemistry, and Ecology of Seasonally Frozen Soils*, US Army Cold Regions Research and Engineering Laboratory, Fairbanks, Alaska, 10–12 June, pp. 537–543.
- French, H.K., Van der Zee, S.E.A.T.M., 1999. Field scale observations of small scale spatial variability of snowmelt drainage and infiltration. *Nordic Hydrol.* 30, 166–176.
- French, H.K., Swensen, B., Englund, J.-O., Meyer, K.-F., 1994. A lysimeter trench for reactive pollutant transport studies. In: Soveri, J., Suokko, T. (Eds.), *Future Groundwater Resources at Risk*, vol. 222. IAHS Publication, pp. 131–138.
- French, H.K., Van der Zee, S.E.A.T.M., Leijnse, A., 1999. Differences in gravity dominated unsaturated flow during autumn rains and snowmelt. *Hydrol. Processes* 13, 2783–2800.
- French, H.K., Van der Zee, S.E.A.T.M., Leijnse, A., 2001. Transport and degradation of propyleneglycol and potassium acetate in the unsaturated zone. *J. Contam. Hydrol.* 49, 23–48.
- French, H.K., Hardbattle, C., Binley, A., Winship, P., Jakobsen, L., 2002. Monitoring snowmelt induced unsaturated flow and transport using electrical resistivity tomography. *J. Hydrol.* 267, 273–284.
- Granger, R.J., Gray, D.M., Dyck, G.E., 1984. Snowmelt infiltration to frozen Prairie soils. *Can. J. Earth Sci.* 21, 669–677.
- Ippisch, O., 2001. Coupled transport in natural porous media, PhD dissertation, Combined Faculties for the Natural Sciences and for Mathematics of the Rupertus Carola University, Heidelberg, Germany, 123 pp.
- Jansson, P.-E., 1991. Simulation model for soil water and heat conditions. Description of the SOIL model. Swedish University of Agricultural Sciences. Department of Soil Sciences. Communications, 91:71, 165 pp.
- Johnsson, H., Lundin, L.-C., 1991. Surface runoff and soil water percolation as affected by snow and soil frost. *J. Hydrol.* 122, 141–159.
- Jørgensen, P., Østmo, S.-R., 1990. Hydrogeology in the Romerike area, southern Norway. *Norges Geologiske Undersøkelse Bull.* 418, 19–26.
- Kjeldset, O., 2002. Ortofotoframstilling fra nærfotogrammetriske skræpptak (Orthophoto production from close range oblique photographs), Master thesis, Department of Mapping Sciences, Agricultural University of Norway, 72 pp.
- LaBrecque, D.J., Miletto, M., Daily, W., Ramirez, A., Owen, E., 1996. The effects of noise on Occam's inversion of resistivity tomography data. *Geophysics* 61, 538–548.
- Langsholt, E., Kitterød, N.-O., Gottschalk, L., 1996. The Moreppen I field site: hydrology and water balance. In: Aagaard, P., Tuttle, K.J. (Eds.), *Proceedings to The Jens-Olaf Englund Seminar, Protection of Groundwater Resources against Contaminants*, 16–18 September, Gardermoen, Oslo University, pp. 9–37.
- Reynolds, J., 1997. *An Introduction to Applied and Environmental Geophysics*. Wiley, New York, 796 pp.
- Stähli, M., Jansson, P.-E., Lundin, L.-C., 1996. Preferential water flow in a frozen soil—a two domain model approach. *Hydrol. Processes* 10, 1305–1316.
- Stähli, M., Jansson, P.-E., Lundin, L.-C., Flüher, H., 1997. Water infiltration and movement in seasonally frozen soils. In: Iskandar, I.K., Wright, E.A., Radke, J.K., Sharratt, B.S., Groenvelt, P.H., Hinzman, L.D. (Eds.), *International Symposium on Physics, Chemistry, and Ecology of Seasonally Frozen Soils*, US Army Cold Regions Research and Engineering Laboratory, Fairbanks, Alaska, 10–12 June, pp. 24–30.
- Telford, W.M., Geldart, L.P., Sheriff, R.E., 1990. *Applied Geophysics*, second ed. Cambridge University Press, Cambridge.
- Tuttle, K., 1997. Sedimentological and Hydrogeological Characterisation of a Raised Ice-Contact Delta—The Preboreal Delta-Complex at Gardermoen, Southeastern Norway, PhD. Thesis, Department of Geology, University of Oslo.
- White, M.D., Oostrom, M., 2000. *Subsurface Transport Over Multiple Phases*, version 2.0, Users guide US Department of Energy and Pacific Northwest National Laboratory, Richland Washington, 238 pp.